

Cs microcell optical reference at 459 nm with short-term frequency stability below 2×10^{-13}

E. Klinger,^{1, a)} C. M. Rivera-Aguilar,^{1, a)} A. Mursa,¹ Q. Tanguy,¹ N. Passilly,¹ and R. Boudot¹
Institut FEMTO-ST, Université Marie et Louis Pasteur, CNRS, SUPMICROTECH, Besançon, France

(*Electronic mail: emmanuel.klinger@femto-st.fr)

(Dated: 31 January 2025)

We describe the short-term frequency stability characterization of external-cavity diode lasers stabilized onto the $6S_{1/2} - 7P_{1/2}$ transition of Cs atom at 459 nm, using a microfabricated vapor cell. The laser beatnote between two nearly-identical systems, each using saturated absorption spectroscopy in a simple retroreflected configuration, exhibits an instability of 2.5×10^{-13} at 1 s, consistent with phase noise analysis, and 3×10^{-14} at 200 s. The primary contributors to the stability budget at 1 second are the FM-AM noise conversion and the intermodulation effect, both emerging from laser frequency noise. These results highlight the potential of microcell-based optical references to achieve stability performances comparable to that of an active hydrogen maser in a remarkably simple architecture.

The optical interrogation of hot alkali atomic vapor within a microfabricated cell has led to the development of high-precision, integrated atomic instruments¹. Pioneers among these devices, chip-scale microwave atomic clocks based on coherent population trapping have achieved remarkable development²⁻⁴, including successful commercialization. These clocks, having a volume of 15–20 cm³, a power consumption of 100–150 mW, and a timing error of a few microseconds per day, are now deployed in navigation systems, instrumentation, metrology, and communications. Nevertheless, their short-term stability is limited by the laser frequency noise while their long-term stability is jeopardized by light-shifts and buffer-gas collisional shifts.

Over the last 20 years, a significant breakthrough in atomic clock performance has been achieved by transitioning from microwave to optical transitions⁵. However, this increase in performance has come in general with a dramatic increase of the complexity, size, and volume. Sub-Doppler spectroscopy (SDS) techniques⁶, that rely on the interaction of a hot atomic vapor confined in a cell with two counter-propagating laser fields, enable the detection of high Q-factor optical atomic resonances. These resonances are well-suited for laser frequency stabilization within a simple-architecture setup that does not require laser cooling.

Optical references based on SDS techniques in cm-scale glass-blown hot vapor cells have demonstrated remarkable stability results. Most projects have involved the spectroscopy of the two-photon transition (TPT) of the Rb atom, at 778 nm⁷⁻¹⁰, or using the 780 nm - 776 nm two-color scheme^{11,12}. Other methods include modulation-transfer spectroscopy¹³ with iodine¹⁴⁻¹⁶, neutral ytterbium-174¹², Rb¹⁷ and Cs atoms¹⁸, or saturated absorption spectroscopy (SAS) in Cs¹⁹ and Rb²⁰ atomic vapors.

With the promising advancements in chip-scale lasers^{21,22}, photonics, and microfabricated vapor cells²³⁻²⁸, SDS techniques become attractive for the demonstration of fully-integrated optical references. For instance, in Ref.²⁹, a

laser was stabilized to a Rb microcell using SAS, reaching a stability below 10^{-11} from 1 to 10^4 s. The photonic integration of a microcell optical clock exploiting TPT of Rb atom at 778 nm was also reported³⁰. Using an external-cavity diode laser (ECDL), it set a record for microcell optical references, achieving a short-term stability of 1.8×10^{-13} at 1 s and 2×10^{-14} after 100 s³¹. Competitive results were also reported with this approach on a transition of ⁸⁷Rb atom³². Dual-frequency sub-Doppler spectroscopy (DFSDS)³³, enabling the detection of high-contrast sign-reversed sub-Doppler resonances, has been used to stabilize an ECDL to a Cs microcell with a stability of 3×10^{-13} at 1 s and below 5×10^{-14} at 100 s³⁴. However, DFSDS requires the generation of a microwave-modulated optical field, usually obtained with an electro-optic modulator, which adds complexity to the system.

Although near-infrared transitions have been mainly used, recent advances in blue and near-ultraviolet integrated lasers³⁵, combined with the two-fold increase of the reference transition frequency, constitute an interesting research path. In this domain, SDS of strontium at 461 nm was recently reported in a micromachined cell³⁶. Nevertheless, strontium needs to be heated to high temperatures ($\sim 300^\circ\text{C}$) to reach a sufficiently high vapor pressure, which poses challenges for maintaining the cell's lifetime. In Ref.³⁷, an ECDL was locked to the $5S_{1/2}(F=2) \rightarrow 6P_{3/2}(F'=3)$ transition of Rb atoms in a tiny cubic cell, yielding a short-term stability of 2.2×10^{-12} at 1 s. Also, the exploration with SAS of the Cs atom $6S_{1/2} \rightarrow 7P_{1/2}$ transition at 459 nm was recently initiated in a microfabricated cell³⁸. However, no frequency stability characterization was reported in this work.

In the present paper, we report the short-term frequency stability characterization of ECDLs stabilized onto the Cs atom $6S_{1/2} \rightarrow 7P_{1/2}$ transition at 459 nm using SAS in a microfabricated vapor cell. In comparison with Ref.³⁸, where separated pump and probe beams were used, we use here SAS in its simplest retro-reflected configuration. Two laser systems were assembled such that a beatnote, obtained by shifting the frequency of one laser with an acousto-optic modulator (AOM), can be analyzed and counted. The Allan deviation of

^{a)}These authors contributed equally.

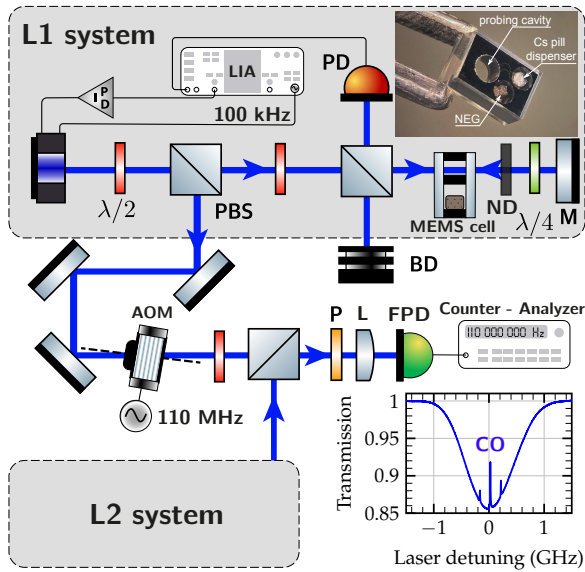


FIG. 1. Experimental setup. Two ECDLs, emitting at 459 nm, are stabilized onto a microfabricated Cs vapor cell, shown in the bottom-right corner, using SAS. The frequency of the laser system 1 (L1) is frequency-shifted by 110 MHz using an acousto-optic modulator (AOM). A laser beatnote between the two lasers, detected at 110 MHz with a fast photodiode (FPD), is filtered, amplified and analyzed. PBS: polarizing beam splitter, BD: beam dump, ND: neutral density filter, M: mirror, PD: photodiode, LIA: lock-in amplifier, PID: PID controller, P: polarizer, L: converging lens.

the laser beatnote, when both lasers are locked, is lower than 2.5×10^{-13} at 1 s and 3×10^{-14} at 200 s. The stability at 1 s of one single laser is then estimated to be 1.8×10^{-13} , a level competitive with best stability results reported so far for MEMS cell-based optical references. The primary factors affecting the short-term stability originate from the laser FM noise, through the FM-AM conversion process and the intermodulation effect³⁹. This suggests that there is room for improvement using lasers with lower FM noise.

Figure 1 shows the experimental setup. Two ECDLs (L1 and L2, Toptica DL-Pro), emitting at 459 nm, are each stabilized onto a Cs vapor microfabricated cell using SAS. An optical isolation stage of 35 dB is placed at the output of the laser head to prevent feedback. The linearly-polarized laser beam crosses a half-wave plate, a polarizing beam splitter (PBS), and is transmitted, as the pump beam ($P_L \simeq 14.3$ mW), through the Cs vapor cell. At the output of the cell are placed a neutral density filter (ND), a quarter-wave plate and a mirror that provides the counter-propagating beam, orthogonally polarized to the incident one, and used as the probe beam ($P_r \simeq 500$ μ W). The reflected beam is then directed by the PBS towards a photodiode (PD) that delivers the spectroscopic signal. The inset of Fig. 1 shows the sub-Doppler resonances detected at the bottom of the Doppler-broadened profile. Due to its higher amplitude, we chose to lock the lasers onto the crossover (CO) line, involved between the $F = 4 \rightarrow 3'$ and $F = 4 \rightarrow 4'$ transitions, separated by 377.6(2) MHz⁴⁰. For laser frequency stabilization, a dispersive zero-crossing error

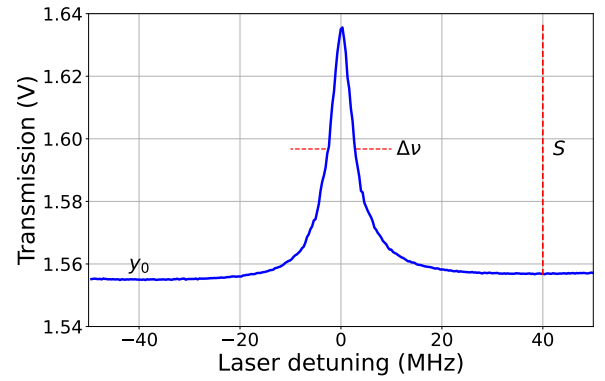


FIG. 2. Central cross-over sub-Doppler resonance used for laser frequency stabilization.

signal is generated from the atomic signal by modulating the laser current (modulation frequency $f_m = 100$ kHz), and applying lock-in detection. The error signal is fed into a digital proportional-integral controller whose output is used to correct the laser current.

The cell technology is adapted from the one described in Ref.³⁸. It involves etching two adjacent cavities in silicon, and enclosing them between two anodically-bonded glass wafers. The first cavity contains a pill dispenser, which is laser-activated after the final sealing in order to fill the cell with Cs vapor^{24,41}. The second cavity, in which atom-light interaction takes place, is 2-mm in diameter and 1.5-mm long, and connected by thin channels to the first cavity. In Ref.³⁸, the zero-power linewidth of the sub-Doppler resonance was measured to be about 8 MHz, which is significantly broader than the transition natural linewidth (~ 950 kHz), with the increase attributed to collisional broadening⁴². In the present work, aiming to enhance the cell purity, a third cavity has been incorporated into the cell preform to host a passive non-evaporable getter (NEG)⁴³, which can also be activated by laser. Additionally, alumino-silicate glass (ASG) is employed for the cell windows in order to minimize helium permeation^{44,45}. The MEMS cell, shown in Fig. 1, is placed within a physics package, controlled at a temperature set-point of about 118°C and covered by a single-layer mu-metal magnetic shield.

For stability characterization, a laser beatnote, obtained between both laser systems by shifting the frequency of the laser 1 with an AOM driven at 110 MHz, was detected, filtered, amplified and sent to a frequency counter (HP53132A) or phase noise analyzer (RS FSWP). The frequency counter was referenced to an active hydrogen maser.

Figure 2 provides a close-up view of the central CO resonance. Fitting the resonance by a Lorentzian function yields a resonance linewidth $\Delta\nu \simeq 6$ MHz, a signal height $S \simeq 76$ mV, a sensitivity $S_l = S/\Delta\nu \simeq 12.6$ mV/MHz, and a contrast $C = S/y_0$, with y_0 the dc background of the resonance line, of 4.8%. Figure 3 shows the evolution of the sub-Doppler resonance signal S , linewidth $\Delta\nu$ and ratio $S/\Delta\nu$ versus the total laser power P_L at the cell input, for laser 1. In these tests, the pump power to probe power ratio $r = P_L/P_r$ is about 27.4. The increase of the pump beam power yields an increase of

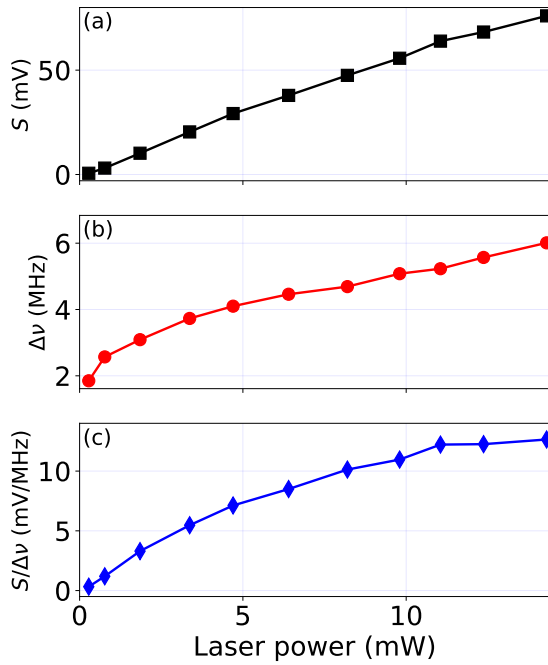


FIG. 3. Signal S (a), linewidth $\Delta\nu$ (b) and signal/linewidth ratio (c) of the sub-Doppler resonance versus the total laser power P_L at the cell input, for laser 1.

the signal S , at the expense of power-broadening of the resonance. At the smallest tested laser power ($P_L \sim 0.28$ mW), we find $\Delta\nu \simeq 1.8$ MHz. This value is significantly smaller than the linewidths reported in³⁸, indicating an improved purity of the cell inner atmosphere. The signal/linewidth ratio increases with the laser power before reaching a plateau at about 15 mW. Similar features were obtained for the laser 2. We chose to operate both laser systems with an incident power $P_L \simeq 14.3$ mW.

Following this spectroscopic study, we have measured the total detection noise at the photodiode (PD) output in different conditions. Results are shown in Fig. 4. The first curve (black) shows the voltage noise of the PD "in the dark" (laser beam blocked). The second curve (red), image of the laser amplitude noise (AM), was measured by tuning the laser frequency out of the Doppler-broadened optical resonance. At $f = f_m = 100$ kHz, the laser AM noise is as low as the photodetector noise, at the level of -130 dBV²/Hz. The last curve (blue) shows the total detection noise measured at half-height of the sub-Doppler resonance. In this case, we observe a clear increase of the noise level, reaching at $f = 100$ kHz the level of -120 dBV²/Hz (i.e. $1 \mu\text{V}/\sqrt{\text{Hz}}$). With the data obtained in Figs. 2 and 4, the signal-to-noise ratio in a 1 Hz bandwidth of the detected resonance is found to be 7.6×10^4 .

Figure 5 shows the phase noise of the laser beatnote, in two conditions. In the free-running case (L1 locked and L2 free), the phase noise of the laser beatnote is -54 dBrad²/Hz, -63 dBrad²/Hz and -78.5 dBrad²/Hz at $f = 100$ kHz, 200 kHz and 1 MHz, respectively. Comparable results were obtained in the case where L1 is free and

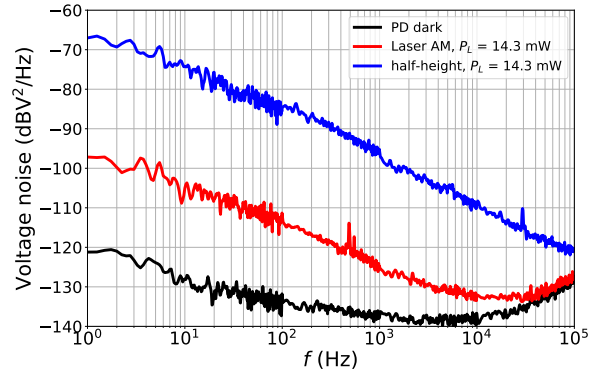


FIG. 4. Detection noise at the photodiode output in different conditions: photodiode in the dark, laser frequency tuned out of the Doppler-broadened optical resonance (laser AM noise), half-height of the sub-Doppler resonance.

L2 is locked. We assume that the phase noise of a single laser is 3 dB lower than the beatnote noise (-66 dBrad²/Hz at $f = 2f_m = 200$ kHz). The contribution σ_{int} of the intermodulation effect³⁹ on the atomic microcell reference stability at 1 s is $\sigma_{int} \simeq \frac{f_m}{\nu_0} \sqrt{S_\phi(2f_m)}$, where ν_0 is the laser frequency ($\nu_0 \simeq 6.5 \times 10^{14}$ Hz) and $S_\phi(2f_m)$ is the phase fluctuations power spectral density of the laser at $f = 2f_m$. Here, with $f_m = 100$ kHz, we estimate $\sigma_{int} \simeq 7.8 \times 10^{-14}$ for a single laser. At $f = 1$ Hz, the phase noise spectrum of the laser beatnote exhibits a f^{-3} slope, signature of flicker frequency noise, with $b_{-3} = +100$ dBrad²/Hz ($+97$ dBrad²/Hz for a single laser), from which a stability

$$\sigma_y(1\text{ s}) = 2 \ln 2 \sqrt{(b_{-3}/\nu_0^2)} = 2.2 \times 10^{-10} \quad (1)$$

can be extracted⁴⁶. In the locked case, the phase noise spectrum of the laser beatnote shows a f^{-2} trend at 1 Hz, signature of white frequency noise, with, $b_{-2} = +45$ dBrad²/Hz ($+42$ dBrad²/Hz for a single laser), from which a stability

$$\sigma_y(1\text{ s}) = \sqrt{(b_{-2}/\nu_0^2)} = 1.9 \times 10^{-13} \quad (2)$$

is expected for a single laser. The bandwidth of the laser frequency servos is about 1.5 kHz in both systems, as revealed by the bumps on the noise spectra.

Figure 6 shows the Allan deviation of the laser beatnote, in free-running and locked conditions. In the free-running case, the fractional frequency stability of the laser beatnote is about 3×10^{-10} at 1 s, in reasonable agreement with the phase noise analysis, and reaches 10^{-9} at 100 s. In locked conditions, the Allan deviation of the laser beatnote is 2.5×10^{-13} at 1 s. Assuming that both lasers contribute equally, the stability of a single laser is estimated to be 1.8×10^{-13} at 1 s. These short-term performances rival the best microcell-based optical references.^{31,34} The Allan deviation plot shows a plateau, possibly caused by the lasers' frequency sensitivity to cell temperature, before averaging down to 3×10^{-14} at 200 s.

The stability budget, reported in Table I and established using the expressions found in⁴⁷, is in good agreement with the

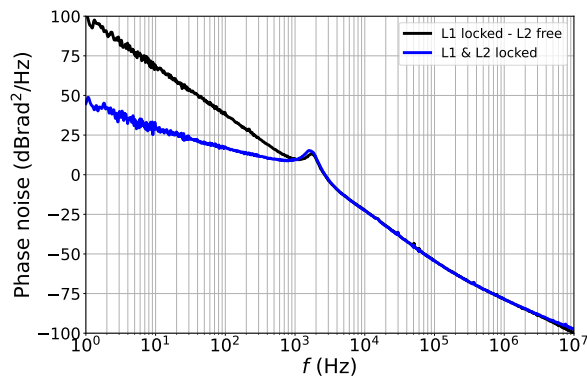


FIG. 5. Phase noise of the laser beatnote in free-running (L1 locked and L2 free) and locked conditions.

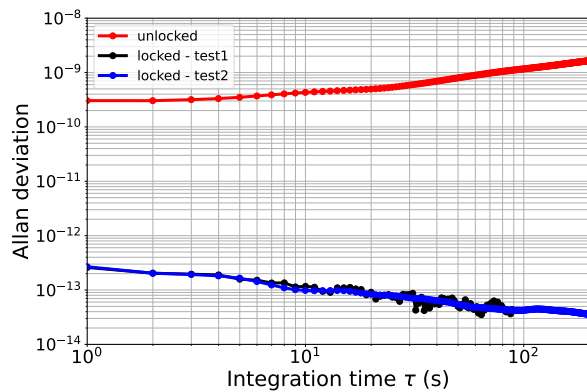


FIG. 6. Allan deviation of the laser beatnote in free-running and locked conditions. Two tests were done in locked conditions giving similar results.

measured stability. The main contribution to the stability at 1 s is currently the FM-AM conversion process, followed by the intermodulation effect. This suggests that the primary factor influencing stability at 1 s is the FM-AM conversion process, followed by the intermodulation effect³⁹. Additional contributions include the laser AM noise and photodetector noise, currently estimated to be in the mid- 10^{-14} range.

In conclusion, we have reported the short-term stability characterization of ECDLs stabilized onto microfabricated cells at 459 nm using SAS of the Cs atom $6S_{1/2}$ - $7P_{1/2}$ transition. The Allan deviation of the laser beatnote between two nearly-identical systems was measured to be 2.5×10^{-13} at 1 s and 3×10^{-14} at 200 s. These performances rival the best stability results reported so far for an optical reference based on a microfabricated cell. The two main contributions to the short-term stability originate from the laser FM noise, through the FM-AM conversion process and the intermodulation effect. This suggests room for improvement with the use of lasers exhibiting lower FM noise⁴⁸.

This work was supported by Centre National d'Etudes Spatiales (CNES), in the frame of the OSCAR project, Agence Nationale de la Recherche (ANR) through LabEX FIRST-TF (Grant ANR 10-LABX-48-01) (LEILA project),

TABLE I. Short-term stability budget of microcell-stabilized laser. The laser power at the photodiode input, used for photon shot noise contribution, is 460 μ W.

Noise source	σ (1 s)
Laser FM-AM noise	1.2×10^{-13}
Intermodulation	7.8×10^{-14}
Laser AM noise	3.8×10^{-14}
PD dark	3.8×10^{-14}
Photon shot noise	8.3×10^{-15}
σ_y (1 s) - single laser	1.6×10^{-13}
σ_y (1 s) - laser beatnote	2.3×10^{-13}

and EIPHI Graduate school (Grant ANR-17-EURE-0002) (REMICS project). The PhD thesis of C. Rivera-Aguilar is co-funded by the program FRANCE2030 QuantEdu (Grant ANR-22-CMAS-0001) and CNES. This work was supported by the French RENATECH network through its FEMTO-ST technological facility (MIMENTO), and by the Oscillator-IMP platform.

DATA AVAILABILITY STATEMENT

The data supporting the findings of this study are available from the corresponding author upon reasonable request.

CONFLICT OF INTEREST

The authors state that there is no conflict of interest to disclose.

- ¹J. Kitching, "Chip-scale atomic devices," *Applied Physics Reviews* **5**, 031302 (2018).
- ²R. Lutwak, A. Rashed, M. Varghese, G. Tepolt, J. LeBlanc, M. J. Mescher, D. K. Serkland, K. M. Geib, G. W. Peake, and S. Romisch, "The Chip-Scale Atomic Clock-Prototype Evaluation," in *Proceedings of the 39th Annual Precise Time and Time Interval Meeting* (Long Beach, CA, 2007) pp. 269–290.
- ³S. Yanagimachi, S. Harasaka, R. Suzuki, M. Suzuki, and S. Goka, "Reducing frequency drift caused by light shift in coherent population trapping-based low-power atomic clocks," *Appl. Phys. Lett.* **116**, 104102 (2020).
- ⁴C. Carlé, M. Abdel Hafiz, S. Keshavarzi, R. Vicarini, N. Passilly, and R. Boudot, "Pulsed-CPT Cs-Ne microcell atomic clock with frequency stability below 2×10^{-12} at 10^5 s," *Optics Express* **31**, 8160–8169 (2023).
- ⁵A. Aeppli, K. Kim, W. Warfield, M. Safranov, and J. Ye, "Clock with 8×10^{-19} systematic uncertainty," *Phys. Rev. Lett.* **123**, 023401 (2024).
- ⁶S. Haroche and F. Hartmann, "Theory of saturated-absorption line shapes," *Phys. Rev. A* **6**, 1280–1300 (1972).
- ⁷K. W. Martin, G. Phelps, N. D. Lemke, M. S. Bigelow, B. Stuhl, M. Wojcik, M. Holt, I. Coddington, M. W. Bishop, and J. H. Burke, "Compact optical atomic clock based on a two-photon transition in rubidium," *Phys. Rev. Appl.* **9**, 014019 (2018).
- ⁸N. D. Lemke, K. W. Martin, R. Beard, B. K. Stuhl, A. J. Metcalf, and J. D. Elgin, "Measurement of optical rubidium clock frequency spanning 65 days," *Sensors* **22**, 1982 (2022).
- ⁹D. Li, K. Liu, P. Wang, and S. Kang, "Dual-interrogation method for suppressing light shift in rb 778 nm two-photon optical frequency standard," *Opt. Express* **32**, 2766–2773 (2024).

- ¹⁰T. Ruelle, E. Batori, S. Kundermann, X. Stehlin, V. Helson, J. Haesler, S. Lecomte, F. Droz, and S. Karlen, "Development of an industrial two-photon Rb atomic clock for timekeeping applications," *Proc. European Frequency Time Forum* (2024).
- ¹¹C. Perrella, P. Light, J. Anstie, F. Baynes, R. White, and A. Luiten, "Dichroic two-photon rubidium frequency standard," *Phys. Rev. Appl.* **12**, 054063 (2019).
- ¹²E. Ahern, J. W. Allison, C. Billington, N. Bourbeau-Hébert, A. P. Hilton, E. Klantsataya, C. Locke, A. N. Luiten, M. Nelligan, R. F. Offer, C. Perrella, S. K. Scholten, B. White, B. M. Sparkes, R. Beard, J. D. Elgin, and K. W. Martin, "Demonstration of a mobile optical clock ensemble at sea," *arXiv*, 2406.03716v2 (2024).
- ¹³D. J. McCarron, S. A. King, and S. L. Cornish, "Modulation transfer spectroscopy in atomic rubidium," *Meas. Sci. Technol.* **19**, 105601 (2008).
- ¹⁴K. Döringshoff, F. Gutsch, V. Schkolnik, C. Kürbis, M. Oswald, B. Pröbster, E. Kovalchuk, A. Bawamia, R. Smol, T. Schuldt, M. Lezius, R. Holzwarth, A. Wicht, C. Braxmaier, M. Krutzik, and A. Peters, "Iodine frequency reference on a sounding rocket," *Phys. Rev. Appl.* **11**, 054068 (2019).
- ¹⁵T. Schuldt, M. Gohlke, M. Oswald, J. Wüst, T. Blomberg, K. Döringshoff, A. Bawamia, A. Wicht, M. Lezius, K. Voss, M. Krutzik, S. Herrmann, E. Kovalchuk, A. Peters, and C. Braxmaier, "Optical clock technologies for global navigation satellite systems," *GPS Solutions* **25**, 83 (2021).
- ¹⁶J. D. Roslund, A. Cingöz, W. D. Lunden, G. B. Partridge, A. S. Kowligy, F. Roller, D. B. Shedy, G. E. Skulason, J. P. Song, J. R. Abo-Shaer, and M. M. Boyd, "Optical clocks at sea," *Nature* **628**, 736–740 (2024).
- ¹⁷S. Lee, G. Moon, S. E. Park, H.-G. Hong, J. H. Lee, S. Seo, T. Y. Kwon, and S.-B. Lee, "Laser frequency stabilization in the 10^{-14} range via optimized modulation transfer spectroscopy on the ^{87}Rb D_2 line," *Opt. Lett.* **48**, 1020–1023 (2023).
- ¹⁸J. Miao, T. Shi, J. Zhang, and J. Chen, "Compact 459-nm cs cell optical frequency standard with $2.1 \times 10^{-13}/\sqrt{\tau}$ short-term stability," *Phys. Rev. Appl.* **18**, 024034 (2022).
- ¹⁹G. D. Rovera, G. Santarelli, and A. Clairon, "A laser diode system stabilized on the caesium d_2 line," *Rev. Sci. Instr.* **65**, 1502–1505 (1994).
- ²⁰C. Affolderbach and G. Mileti, "Tuneable, stabilised diode lasers for compact atomic frequency standards and precision wavelength references," *Optics and Lasers in Engineering* **43**, 291–302 (2005).
- ²¹M. Corato-Zanarella, A. Gil-Molina, X. Ji, M. C. Shin, A. Mohanty, and M. Lipson, "Widely tunable and narrow-linewidth chip-scale lasers from near-ultraviolet to near-infrared wavelengths," *Nat. Photonics* **17**, 157–164 (2023).
- ²²A. Isichenko, A. S. Hunter, D. Bose, N. Chauhan, M. Song, K. Liu, M. W. Harrington, and D. J. Blumenthal, "Sub-Hz fundamental, sub-kHz integral linewidth self-injection locked 780 nm hybrid integrated laser," *Scientific Reports* **14**, 27015 (2024).
- ²³J. Kitching, S. Knappe, and L. Hollberg, "Miniature vapor-cell atomic-frequency references," *Applied Physics Letters* **81**, 553–555 (2002).
- ²⁴A. Douahi, L. Nieradko, J.-C. Beugnot, J. A. Dziuban, E. Maillote, S. Guérandel, M. Moraja, C. Gorecki, and V. Giordano, "Vapour microcell for chip scale atomic frequency standard," *Electronics Letters* **43**, 279–280 (2007).
- ²⁵D. G. Bopp, V. M. Maurice, and J. E. Kitching, "Wafer-level fabrication of alkali vapor cells using in-situ atomic deposition," *Journal of Physics: Photonics* **3**, 015002 (2020).
- ²⁶V. Maurice, C. Carlé, S. Keshavarzi, R. Chutani, S. Queste, L. Gauthier-Manuel, J.-M. Cote, R. Vicarini, M. Abdel Hafiz, R. Boudot, and N. Passilly, "Wafer-level vapor cells filled with laser-actuated hermetic seals for integrated atomic devices," *Microsystems & Nanoengineering* **8**, 129 (2022).
- ²⁷S. Dyer, P. F. Griffin, A. Arnold, F. Mirando, D. P. Burt, E. Riis, and J. P. McGilligan, "Micro-machined deep silicon atomic vapor cells," *J. Appl. Phys.* **132**, 134401 (2022).
- ²⁸V. G. Lucivero, A. Zanon, G. Corrielli, R. Osellame, and M. W. Mitchell, "Laser-written vapor cells for chip-scale atomic sensing and spectroscopy," *Opt. Express* **30**, 27149–27163 (2022).
- ²⁹M. Hummon, S. Kang, D. Bopp, D. Westly, S. Kim, C. Fredrick, S. Diddams, K. Srinivasan, V. Aksyuk, and J. Kitching, "Photonic chip for laser stabilization to an atomic vapor with 10^{-11} instability," *Optica* **5**, 443–449 (2018).
- ³⁰Z. L. Newman, V. Maurice, T. Drake, J. R. Stone, T. C. Briles, D. T. Spencer, C. Fredrick, Q. Li, D. Westly, B. R. Ilic, B. Shen, M.-G. Suh, K. Y. Yang, C. Johnson, D. M. S. Johnson, L. Hollberg, K. J. Vahala, K. Srinivasan, S. A. Diddams, J. Kitching, S. B. Papp, and M. T. Hummon, "Architecture for the photonic integration of an optical atomic clock," *Optica* **6**, 680–685 (2019).
- ³¹Z. L. Newman, V. N. Maurice, C. D. Fredrick, T. M. Fortier, H. Leopardi, L. Hollberg, S. A. Diddams, J. E. Kitching, and M. T. Hummon, "High-performance, compact optical standard," *Optics Letters* **46**, 4702–4705 (2021).
- ³²M. Callejo, A. Mursa, R. Vicarini, E. Klinger, J. Millo, N. Passilly, and R. Boudot, "Short-term stability of a microcell optical reference based on the Rb atom two-photon transition at 778 nm," *J. Opt. Soc. Am. B* **42**, 151–158 (2025).
- ³³M. Abdel Hafiz, G. Coget, E. Clercq, and R. Boudot, "Doppler-free spectroscopy on the cs d_1 line with a dual-frequency laser," *Opt. Lett.* **41**, 2982–2985 (2016).
- ³⁴A. Gusching, J. Millo, I. Ryger, R. Vicarini, M. Abdel Hafiz, N. Passilly, and R. Boudot, "Cs microcell optical reference with frequency stability in the low 10^{-13} range at 1 s," *Opt. Lett.* **48**, 1526–1529 (2023).
- ³⁵A. Siddharth, T. Wunderer, G. Lihachev, A. S. Voloshin, C. Haller, R. N. Wang, M. Teepe, Z. Yang, J. Liu, J. Riemensberger, N. Grandjean, N. Johnson, and T. J. Kippenberg, "Near ultraviolet photonic integrated lasers based on silicon nitride," *APL Photonics* **7**, 046108 (2022).
- ³⁶J. M. Pate, J. Kitching, and M. T. Hummon, "Microfabricated strontium atomic vapor cells," *Optics letters* **48**, 383–386 (2023).
- ³⁷A. Zhang, Y. Zhang, W. Zhao, Y. Tian, Y. Zhang, S. Gu, and J. Chen, "Exploration of a vapor cell optical frequency standard scheme implemented using doppler-free spectroscopy," *Opt. Lett.* **49**, 5475–5478 (2024).
- ³⁸E. Klinger, A. Mursa, C. M. Rivera-Aguilar, R. Vicarini, N. Passilly, and R. Boudot, "Sub-doppler spectroscopy of the cs atom $6S_{1/2}$ – $7P_{1/2}$ transition at 459 nm in a microfabricated vapor cell," *Optics Letters* **49**, 1953 (2024).
- ³⁹C. Audoin, V. Candelier, and N. Dimarcq, "A limit to the frequency stability of passive frequency standards due to an intermodulation effect," *IEEE Trans. Instr. Meas.* **40**, 121–125 (1991).
- ⁴⁰W. D. Williams, M. T. Herd, and W. B. Hawkins, "Spectroscopic study of the $7P_{1/2}$ and $7P_{3/2}$ states in cesium-133," *Laser Physics Letters* **15**, 095702 (2018).
- ⁴¹R. Vicarini, V. Maurice, M. Abdel Hafiz, J. Rutkowski, C. Gorecki, N. Passilly, L. Ribetto, V. Gaff, V. Volant, S. Galliou, and R. Boudot, "Demonstration of the mass-producible feature of a Cs vapor microcell technology for miniature atomic clocks," *Sensors and Actuators A: Physical* **280**, 99–106 (2018).
- ⁴²G. A. Pitz, D. E. Wertepny, and G. P. Perram, "Pressure broadening and shift of the cesium D_1 transition by the noble gases and N_2 , H_2 , HD, D_2 , CH_4 , C_2H_6 , CF_4 , and ^3He ," *Phys. Rev. A* **80**, 062718 (2009).
- ⁴³R. Boudot, J. P. McGilligan, K. Moore, V. Maurice, G. D. Martinez, A. Hansen, E. de Clercq, and J. E. Kitching, "Enhanced observation time of magneto-optical traps using micro-machined non-evaporable getter pumps," *Scientific Reports* **10**, 16590 (2020).
- ⁴⁴A. T. Dellis, V. Shah, E. A. Donley, S. Knappe, and J. E. Kitching, "Low helium permeation cells for atomic microsystems technology," *Optics letters* **41**, 2775–2778 (2016).
- ⁴⁵C. Carlé, S. Keshavarzi, A. Mursa, P. Karvinen, R. K. Chutani, S. Bargiel, S. Queste, R. Vicarini, P. Abbé, M. Abdel Hafiz, V. Maurice, R. Boudot, and N. Passilly, "Reduction of helium permeation in microfabricated cells using aluminosilicate glass substrates and Al_2O_3 coatings," *J. Appl. Phys.* **133** (2023).
- ⁴⁶E. Rubiola, *Phase Noise and Frequency Stability in Oscillators*, The Cambridge RF and Microwave Engineering Series (Cambridge University Press, 2008).
- ⁴⁷A. Gusching, M. Petersen, N. Passilly, D. Brazhnikov, M. Abdel Hafiz, E. de Clercq, and R. Boudot, "Short-term stability of Cs microcell-stabilized lasers using dual-frequency sub-Doppler spectroscopy," *Journal of the Optical Society of America B* **38**, 3254–3260 (2021).
- ⁴⁸R. Kervazo, G. Perin, A. Congar, L. Lablonde, R. Butté, N. Grandjean, L. Bodiou, J. Charrier, and S. Trebaol, "Sub-20 khz low-frequency noise near ultraviolet butt-coupled fiber bragg grating external cavity laser diode," *Appl. Phys. Lett.* **125** (2024).